# On Galerkin approximations of the surface-active quasigeostrophic equations

Cesar B. Rocha* and William R. Young

*Scripps Institution of Oceanography, University of California, San Diego, La Jolla, California*

Ian Grooms†

*Center for Atmosphere Ocean Science, Courant Institute of Mathematical Sciences, New York University, New York, New York*

**Corresponding author address:* Cesar B. Rocha, Scripps Institution of Oceanography, University of California, San Diego, 9500 Gilman Dr. MC 0213, La Jolla, CA 92093

E-mail: crocha@ucsd.edu

†Current affiliation: Department of Applied Mathematics, University of Colorado, Boulder, Colorado

# ABSTRACT

We study the representation of solutions of the three-dimensional quasi-geostrophic (QG) equations using Galerkin series with standard vertical modes, with particular attention to the incorporation of active surface buoyancy dynamics. We extend two existing Galerkin approaches (A and B) and develop a new Galerkin approximation (C). Approximation A, due to Flierl (1978), represents the streamfunction as a truncated Galerkin series and defines the potential vorticity (PV) that satisfies the inversion problem exactly. Approximation B, due to Tulloch and Smith (2009), represents the PV as a truncated Galerkin series and calculates the streamfunction that satisfies the inversion problem exactly. Approximation C, the true Galerkin approximation for the QG equations, represents both streamfunction and PV as truncated Galerkin series, but does not satisfy the inversion equation exactly. The three approximations are fundamentally different unless the boundaries are isopycnal surfaces. We discuss the advantages and limitations of approximations A, B, and C in terms of mathematical rigor and conservation laws, and illustrate their relative efficiency by solving linear stability problems with nonzero surface buoyancy. With moderate number of modes, B and C have have superior accuracy than A at high wavenumbers. Because B lacks conservation of energy, we recommend approximation C for constructing solutions to the surface-active QG equations using Galerkin series with standard vertical modes.

## 1. Introduction

Recent interest in upper-ocean dynamics and sub-mesoscale turbulence has focussed attention on surface geostrophic dynamics and the role of surface buoyancy variations. A main issue is the representation of active surface buoyancy by finite vertical truncations of the quasigeostrophic (QG) equations. Standard multi-layer (e.g., Pedlosky 1987) and modal approximations (e.g., Flierl 1978) assume that there is no variation of buoyancy on the surfaces.

Only few attempts have being made to represent both surface active and interior dynamics in the QG equations. The pioneering work by Tulloch and Smith (2009) developed a "two-mode two-surface" model that represents the surface dynamics exactly and approximates the interior dynamics using the barotropic and first baroclinic modes. The interaction of surface and interior dynamics motivated the development a new set of vertical modes that simultaneously diagonalize energy and a linear combination of enstrophy and surface buoyancy variance (Smith and Vanneste 2013). Other studies of the interaction of surface and interior dynamics avoid vertical modes and use instead finite-difference schemes (Roullet et al. 2012) or idealize the interior potential vorticity as a delta-function sheet (Callies et al. 2015).

Here we explore the representation of surface and interior dynamics using the familiar vertical modes of physical oceanography. These "standard modes", denoted here by $\mathsf{p}_n(z)$, are defined by the Sturm-Liouville eigenproblem

$$\frac{\mathrm{d}}{\mathrm{d}z}\frac{f_0^2}{N^2}\frac{\mathrm{d}\mathsf{p}_n}{\mathrm{d}z} = -\kappa_n^2\mathsf{p}_n\,, \tag{1}$$

with homogeneous Neumann boundary conditions at the bottom ($z = z^-$) and top ($z = z^+$) surfaces of the domain:

$$\frac{\mathrm{d}\mathsf{p}_n}{\mathrm{d}z}\left(z^{\pm}\right) = 0\,. \tag{2}$$

In (1) $N(z)$ is the buoyancy frequency and $f_0$ is the Coriolis parameter. The eigenvalue $\kappa_n$ in (1) is the deformation wavenumber of the $n$'th mode. With normalization, the modes satisfy the orthogonality condition

$$\frac{1}{h}\int_{z^-}^{z^+} \mathsf{p}_n \mathsf{p}_m \,\mathrm{d}z = \delta_{mn}\,, \tag{3}$$

where $h \stackrel{\text{def}}{=} z^+ - z^-$ is the depth. The barotropic mode is $\mathsf{p}_0 = 1$ and $\kappa_0 = 0$.

The modes defined by the eigenproblem (1) and (2) provide a fundamental basis for representing solutions of both the primitive and quasigeostrophic equations as a linear combination of $\{\mathsf{p}_n\}$ (Gill 1982; Pedlosky 1987; Vallis 2006; Ferrari and Wunsch 2010; LaCasce 2012). In fact, the set $\{\mathsf{p}_n\}$ is mathematically complete and can be used to represent *any* field with finite square integral,

$$\int_{z^-}^{z^+} f^2 \,\mathrm{d}z < \infty\,. \tag{4}$$

Even if the function $f(z)$ has nonzero derivative at $z^{\pm}$, or internal discontinuities, its representation as a linear combination of the basis functions $\{\mathsf{p}_n\}$ converges in $L^2(z^-, z^+)$ i.e., the integral of the squared error goes to zero as the number of basis functions increases (e.g., Hunter and Nachtergaele 2001, ch. 10). In quasigeostrophic dynamics both the streamfunction $\psi$ and the potential vorticity (PV) $q$ satisfy the requirement (4) and thus both $\psi$ and $q$ can be effectively represented by linearly combining $\{\mathsf{p}_n\}$.

Despite the rigorous assurance of completeness in the previous paragraph, the utility of $\{\mathsf{p}_n\}$ for problems with nonuniform surface buoyancy has been questioned by several authors (e.g., Lapeyre 2009; Roullet et al. 2012; Smith and Vanneste 2013). These authors argue that the homogeneous boundary conditions in (2) are incompatible with nonzero surface buoyancy and that representation of the streamfunction $\psi$ as a linear combination of $\{\mathsf{p}_n\}$ is useless if $\psi_z$ is nonzero on the surfaces.

The aim of this paper is to obtain a good Galerkin approximation to solutions of the QG equation with nonzero surface buoyancy using the familiar basis $\{\mathsf{p}_n\}$. We show that that both the inversion problem *and* evolutionary dynamics can be handled using $\{\mathsf{p}_n\}$ to represent the streamfunction. As part of this program we revisit and extend two existing modal approximations (Flierl 1978; Tulloch and Smith 2009), and develop a new Galerkin approximation. We discuss the relative merit of the three approximations in terms of their mathematical rigor and conservation laws, and illustrate their efficiency and caveats by solving linear stability problems with nonzero surface buoyancy.

Using concrete examples, we show that the concerns expressed by earlier authors regarding the suitability of the standard modes $\{\mathsf{p}_n\}$ are over-stated: even with nonzero surface buoyancy, the Galerkin expansion of the streamfunction $\psi$ in terms of $\{\mathsf{p}_n\}$ converges absolutely and uniformly with no Gibbs phenomena, and the same is true for the potential vorticity $q$. A modest number of terms provides a good approximation to $\psi$ and $q$ throughout the domain, including on the top and bottom boundaries. In other words, the surface streamfunction can be expanded in terms of $\{\mathsf{p}_n\}$ and, with enough modes, this representation can then be used to accurately calculate the advection of nonzero surface buoyancy. In section 5 we illustrate this procedure by solving the classic Eady problem using the basis $\{\mathsf{p}_n\}$ for the streamfunction.

## 2. The exact system

In this section we summarize the basic properties of the QG system. For a detailed derivation see Pedlosky (1987).

### a. Formulation

The streamfunction is denoted $\psi(x,y,z,t)$ and we use the following notation.

$$u = -\psi_y\,, \qquad v = \psi_x\,, \qquad \vartheta = \left(\frac{f_0}{N}\right)^2 \psi_z\,. \tag{5}$$

The variable $\vartheta$ is related to the buoyancy by $b = N^2\vartheta/f_0$. The QG potential vorticity (QGPV) equation is

$$\partial_t q + \mathsf{J}(\psi, q) + \beta v = 0\,, \tag{6}$$

where the potential vorticity is

$$q = (\triangle + \mathsf{L})\,\psi\,, \tag{7}$$

with

$$\triangle \stackrel{\text{def}}{=} \partial_x^2 + \partial_y^2\,, \qquad \text{and} \qquad \mathsf{L} \stackrel{\text{def}}{=} \partial_z \left(\frac{f_0}{N}\right)^2 \partial_z\,. \tag{8}$$

Also in (6), the Jacobian is $\mathsf{J}(A,B) \stackrel{\text{def}}{=} \partial_x A\,\partial_y B - \partial_y A\,\partial_x B$.

The boundary conditions at the top ($z = z^+$) and bottom ($z = z^-$) are that $w = 0$, or equivalently

$$@z = z^{\pm}: \qquad \partial_t \vartheta^{\pm} + \mathsf{J}(\psi^{\pm}, \vartheta^{\pm}) = 0\,. \tag{9}$$

Above we have used the superscripts $+$ and $-$ to denote evaluation at $z^+$ and $z^-$ e.g., $\psi^+ = \psi(x,y,z^+,t)$.

### b. Quadratic conservation laws

In the absence of sources and sinks, the exact QG system has four quadratic conservation laws: energy, potential enstrophy, and surface buoyancy variance at the two surfaces (e.g., Pedlosky 1987; Vallis 2006). Throughout we assume horizontal periodic boundary conditions.

The well-known energy conservation law is

$$\frac{d}{dt}\underbrace{\int \tfrac{1}{2}|\boldsymbol{\nabla}\psi|^2 + \tfrac{1}{2}\left(\tfrac{f_0}{N}\right)^2 (\partial_z\psi)^2 \, \mathrm{d}V}_{\stackrel{\text{def}}{=}E} = 0\,. \tag{10}$$

The total energy is $\rho_0 E$, where $\rho_0$ is a reference density.

If $\beta = 0$ then there are many quadratic potential enstrophy invariants: the volume integral of $q^2 A(z)$, with $A(z)$ an arbitrary function of the vertical coordinate, is conserved. The choice $A(z) = \delta(z - z_*)$ reduces to conservation of the surface integral of $q^2$ at any level $z_*$.

Charney (1971) noted that, in a doubly periodic domain, nonzero $\beta$ destroys all these quadratic potential enstrophy conservation laws, including the conservation of potential enstrophy defined simply as the volume integral of $q^2$. Multiplying the QGPV equation (6) by $q$, and integrating by parts, we obtain

$$\frac{\mathrm{d}}{\mathrm{d}t}\int \tfrac{1}{2}q^2 \, \mathrm{d}V + \beta \int \left[v\vartheta\right]_{z^-}^{z^+} \mathrm{d}S = 0\,. \tag{11}$$

The potential enstrophy equation (11) is the finite-depth analog of equation (13) in Charney's paper. To make progress Charney assumed $\vartheta = 0$ at the ground. But the $\beta$-term on the right of (11) can be eliminated by cross-multiplying the QGPV equation (6) evaluated at the surfaces $z^{\pm}$ with the boundary conditions (9), and combining with (11). Thus, in a doubly periodic domain, nonzero $\beta$ selects a uniquely conserved potential enstrophy from the infinitude of $\beta = 0$ potential enstrophy conservation laws:

$$\frac{d}{dt}\underbrace{\int \tfrac{1}{2}q^2 \, \mathrm{d}V - \int q^+\vartheta^+ - q^-\vartheta^- \, \mathrm{d}S}_{\stackrel{\text{def}}{=}Z} = 0\,. \tag{12}$$

With $\beta \neq 0$ the surface contributions in (12) are required to form a conserved quadratic quantity involving $q^2$. Notice that Z is not sign-definite. To our knowledge, the conservation law in (12) is previously unremarked.

Finally, in addition to $E$ and $Z$, the surface buoyancy variance is conserved on each surface

$$\frac{\mathrm{d}}{\mathrm{d}t}\int \tfrac{1}{2}\left(\vartheta^{\pm}\right)^2 \mathrm{d}S = 0\,. \tag{13}$$

Thus, with $\beta \neq 0$, the QG model has four quadratic conservation laws: $E$, $Z$ and the buoyancy variance at the two surfaces.

## 3. Galerkin approximation using standard vertical modes

A straightforward approach is to represent the streamfunction by linearly combining the first $\mathrm{N}+1$ vertical modes. The mean square error in this approximation is

$$\mathrm{err}_{\psi}(a_0, a_1, \cdots a_{\mathrm{N}}) \stackrel{\text{def}}{=} \frac{1}{h}\int_{z^-}^{z^+} \left(\psi - \sum_{n=0}^{\mathrm{N}} a_n \mathsf{p}_n\right)^2 \mathrm{d}z\,. \tag{14}$$

We use a roman font, and context, to distinguish the truncation index N in (14) from the buoyancy frequency $N(z)$. The coefficients $a_0$ through $a_{\mathrm{N}}$ are determined to minimize $\mathrm{err}_{\psi}$, and thus one obtains the Galerkin approximation $\psi_{\mathrm{N}}^{\mathrm{G}}$ to the exact streamfunction:

$$\psi_{\mathrm{N}}^{\mathrm{G}}(x,y,z,t) \stackrel{\text{def}}{=} \sum_{n=0}^{\mathrm{N}} \breve{\psi}_n(x,y,t)\mathsf{p}_n(z)\,, \tag{15}$$

where the coefficients in the sum above are

$$\breve{\psi}_n(x,y,t) \stackrel{\text{def}}{=} \tfrac{1}{h}\int_{z^-}^{z^+} \psi\, \mathsf{p}_n\, \mathrm{d}z\,. \tag{16}$$

Throughout we use the superscript $\breve{}$ to denote a Galerkin coefficient defined via projection of a field onto a vertical mode.

In complete analogy with the streamfunction, one can also develop an $(\mathrm{N}+1)$-mode Galerkin approximation to the PV:

$$q_{\mathrm{N}}^{\mathrm{G}}(x,y,z,t) \stackrel{\text{def}}{=} \sum_{n=0}^{\mathrm{N}} \breve{q}_n(x,y,t)\mathsf{p}_n(z)\,, \tag{17}$$

with coefficients

$$\breve{q}_n \stackrel{\text{def}}{=} \tfrac{1}{h}\int_{z^-}^{z^+} q\, \mathsf{p}_n\, \mathrm{d}z\,. \tag{18}$$

The construction of the Galerkin approximation $q_{\mathrm{N}}^{\mathrm{G}}$ above minimizes a mean square error $\mathrm{err}_q$ defined in analogy with (14).

Now recall that the exact $\psi$ and $q$ are related by the elliptic "inversion problem":

$$(\triangle + \mathsf{L})\psi = q\,, \tag{19}$$

with boundary conditions at $z^{\pm}$:

$$\left(\frac{f_0}{N}\right)^2 \psi_z = \vartheta^{\pm}\,. \tag{20}$$

The Galerkin approximations in (15) through (18) are defined independently of the information in (19) and (20). The relationship between the Galerkin coefficients $\breve{q}_n$ and $\breve{\psi}_n$ is obtained by multiplying (19) by $\frac{1}{h}\mathsf{p}_n(z)$ and integrating over the depth. Noting the intermediate result

$$\frac{1}{h}\int_{z^-}^{z^+} \mathsf{p}_n \mathsf{L}\psi\,\mathrm{d}z = \frac{1}{h}\left[\mathsf{p}_n^+\vartheta^+ - \mathsf{p}_n^-\vartheta^-\right] - \kappa_n^2\breve{\psi}_n\,, \tag{21}$$

we obtain

$$\breve{q}_n = \triangle_n\breve{\psi}_n + \underbrace{\frac{1}{h}\left(\mathsf{p}_n^+\vartheta^+ - \mathsf{p}_n^-\vartheta^-\right)}_{\text{surface terms}}, \tag{22}$$

where $\triangle_n$ is the $n$'th mode Helmholtz operator

$$\triangle_n \stackrel{\text{def}}{=} \triangle - \kappa_n^2\,. \tag{23}$$

The relation in (22) is the key to a good Galerkin approximation to surface-active quasigeostrophic dyamics.

Term-by-term differentiation of the $\psi_{\mathrm{N}}^{\mathrm{G}}$-series in (15) does not give the $q_{\mathrm{N}}^{\mathrm{G}}$ series in (17) unless $\vartheta^{\pm} = 0$. In other words, term-by-term differentiation does not produce the correct relation (22) between $\breve{q}_n$ and $\breve{\psi}_n$. Thus the Galerkin truncated PV and the Galerkin truncated streamfunction do not satisfy the inversion boundary value problem exactly

$$(\triangle + \mathsf{L})\,\psi_{\mathrm{N}}^{\mathrm{G}} \neq q_{\mathrm{N}}^{\mathrm{G}}\,. \tag{24}$$

Despite (24), the truncated series $\psi_{\mathrm{N}}^{\mathrm{G}}$ and $q_{\mathrm{N}}^{\mathrm{G}}$ are the best least-squares approximations to $\psi$ and $q$.

Notice that, in analogy with the Galerkin approximations for $q$ and $\psi$,

$$\breve{\delta}_n^+ = \tfrac{1}{h}\mathsf{p}_n^+ \qquad \text{and} \qquad \breve{\delta}_n^- = \tfrac{1}{h}\mathsf{p}_n^- \,, \tag{25}$$

where

$$\delta_{\mathrm{N}}^{+G}(z) = \sum_{n=0}^{\mathrm{N}} \breve{\delta}_n^+ \mathsf{p}_n \qquad \text{and} \qquad \delta_{\mathrm{N}}^{-G}(z) = \sum_{n=0}^{\mathrm{N}} \breve{\delta}_n^- \mathsf{p}_n \,, \tag{26}$$

are finite approximations to distributions $\delta(z - z^{\pm})$ at the surfaces. Of course, these surface $\delta$-distributions do not satisfy the $L^2$ convergence condition in (4) and thus the series in (26) only converge in a distributional sense (e.g., Hunter and Nachtergaele 2001). For instance, if $f$ satisfies the $L^2$ convergence condition in (4), then

$$\int_{z^-}^{z^+} f(z)\delta_{\mathrm{N}}^{+G}(z)\,\mathrm{d}z \;\to\; \int_{z^-}^{z^+} f(z)\delta(z - z^+)\,\mathrm{d}z = f(z^+)\,, \tag{27}$$

as $\mathrm{N} \to \infty$. Thus, in that limit,

$$\big(\triangle + \mathsf{L}\big)\,\psi_{\mathrm{N}}^{\mathrm{G}} \rightharpoonup q - \delta(z - z^+)\,\vartheta^+ + \delta(z - z^-)\,\vartheta^- \,, \tag{28}$$

where $\rightharpoonup$ denotes distributional convergence. The right-hand-side of (28) is the Brethertonian modified potential vorticity (Bretherton 1966) with the boundary conditions incorporated as PV sheets. To illustrate (24) and (28) we present an elementary example that is is relevant to our discussion of the Eady problem in section 5.

*An elementary example: the Eady basic state*

As an example, consider the case with constant buoyancy frequency $N$. We use nondimensional units so that the surfaces are at $z^- = -1$ and $z^+ = 0$. The standard vertical modes are $\mathsf{p}_0 = 1$ and, for $n \geq 1$

$$\mathsf{p}_n = \sqrt{2}\cos(n\pi z)\,, \tag{29}$$

with $\kappa_n = n\pi$.

We consider the basic state of the Eady problem with streamfunction

$$\psi = -\underbrace{(1+z)}_{U}\, y\,, \tag{30}$$

and zero interior PV $q = 0$ and $\beta = 0$. The surface buoyancies are $\vartheta^{\pm} = -y$.

The Galerkin expansion of the PV $q = 0$ is exact: $\breve{q}_{\mathrm{N}} = 0$ and therefore $q^{\mathrm{G}}_{\mathrm{N}} = 0$. The truncated Galerkin expansion of $\psi$ follows from either (16) or (22) and is

$$\psi^{\mathrm{G}}_{\mathrm{N}} = -\underbrace{\left[\tfrac{1}{2}\mathsf{p}_0 + 2\sqrt{2}\left(\frac{\mathsf{p}_1}{\pi^2} + \frac{\mathsf{p}_3}{(3\pi)^2} + \cdots + \frac{\mathsf{p}_{\mathrm{N}}}{(\mathrm{N}\pi)^2}\right)\right]}_{U^{\mathrm{G}}_{\mathrm{N}}} y\,. \tag{31}$$

(We assume that N is odd, so that the last term in the truncated series is as above.) Despite the nonzero derivative of $\psi$ at the boundaries, the series in (31) is absolutely and uniformly convergent on the closed interval $-1 \le z \le 0$. The $\mathrm{N}^{-2}$ behavior of the series (31) ensures uniform convergence, e.g., using the M-test (Hunter and Nachtergaele 2001). There are no Gibbs oscillations and a modest number of terms provides a good approximation to the base velocity $U$ (Figure 1a). All these desirable properties are lost if we differentiate (31) with respect to $z$.

Thus, to illustrate (24) and (28), notice that if one attempts to calculate the Eady PV, namely $q = 0$, by direct differentiation of (31), one obtains

$$(\triangle + \mathsf{L})\, \psi^{\mathrm{G}}_{\mathrm{N}} = 2\sqrt{2}\,(\mathsf{p}_1 + \mathsf{p}_3 + \cdots \mathsf{p}_{\mathrm{N}})\, y \tag{32}$$

$$= 2\,\frac{\sin\left[(\mathrm{N}+1)\pi z\right]}{\sin(\pi z)}\, y\,. \tag{33}$$

The series (32) does not converge in a pointwise sense and the partial sum is violently oscillatory as $\mathrm{N} \to \infty$. However, in a distributional sense (Hunter and Nachtergaele 2001, ch. 11), the exact sum in (33) does converge to $\delta$-distributions on the boundaries; see figures 1(b) and 1(c). These boundary $\delta$-distributions are the Brethertonian PV sheets (Bretherton 1966). To some extent, which we investigate in section 5(a), the series (32) is rescued by this Brethertonian interpretation.

Of course the correct Galerkin approximation to the Eady PV $q = 0$ is the splendidly convergent series $0 = 0\mathsf{p}_0 + 0\mathsf{p}_1 + \cdots$, which is obtained if one uses either (18) or (22) to obtain $\breve{q}_n = 0$. This seemingly trivial example illustrates potentially confusing issues which arise if one differentiates a Galerkin approximation: the standard modes provide good representations of $\psi$ and $q$, even if $\psi_z$ is nonzero on the boundaries. The problem is that differentiating the $\psi$-series to produce a $q$-series does not produce the Galerkin approximation to $q$.

## 4. Three approximations

In (24) we noted that the Galerkin approximations to $\psi$ and $q$ do not exactly satisfy the inversion relation. To address this error there are at least three different approximations one can make. The three approximations are equivalent when $\vartheta^{\pm} = 0$. In the next three sub-sections, we provide a detail description of each approximation. After testing, we recommend approximation C as the most reliable approximation using standard vertical modes.

### *a. Approximation A*

Approximation A uses the truncated series $\psi_{\mathrm{N}}^{\mathrm{G}}$ in (15) as a least-squares Galerkin approximation to the streamfunction $\psi$. A does not use the Galerkin approximation for $q$. Instead, the approximate PV, $q_{\mathrm{N}}^{A}(x, y, z, t)$, is *defined* so that the interior inversion relation is satisfied exactly:

$$q_{\mathrm{N}}^{A} \overset{\mathrm{def}}{=} \left(\triangle + \mathsf{L}\right) \psi_{\mathrm{N}}^{\mathrm{G}} . \tag{34}$$

This is the approximation introduced by Flierl (1978) in a context without surface buoyancy, and it is now regarded as the standard in physical oceanography. Note that $q_{\mathrm{N}}^{A}$ in (34) is not the least-squares approximation to the exact $q$. Instead the series $q_{\mathrm{N}}^{A}$ is obtained using term-by-term differentiation of the series $\psi_{\mathrm{N}}^{\mathrm{G}}$. The example surrounding (32) shows that with nonzero surface buoyancy, the approximation $q_{\mathrm{N}}^{A}$ is strongly oscillatory in the interior of the domain and approaches the Brethertonian PV on the right of (28) as $\mathrm{N} \to \infty$. The rapid interior oscillation of $q_{\mathrm{N}}^{A}$ is a spurious creation of term-by- term differentiation. Later, in section 5, these spurious oscillations will produce significant errors in the solution of the Eady stability problem.

Following Flierl (1978), in approximation A the N-mode approximate PV is defined via (34) and, using the modal representation for $\psi_{\mathrm{N}}^{\mathrm{G}}$ in (15), this is equivalent to

$$q_{\mathrm{N}}^{A} \stackrel{\text{def}}{=} \sum_{n=0}^{\mathrm{N}} \triangle_n \breve{\psi}_n(x,y,t)\, \mathsf{p}_n(z)\,, \tag{35}$$

where $\triangle_n$ is the Helmholtz operator in (23). Following the appendix of Flierl (1978), one can use Galerkin projection of the nonlinear evolution equation (6) onto the modes $\mathsf{p}_n$ to obtain $\mathrm{N}+1$ evolution equations for the coefficients $\breve{\psi}_n$:

$$\partial_t \triangle_n \breve{\psi}_n + \sum_{m=0}^{\mathrm{N}} \sum_{s=0}^{\mathrm{N}} \Xi_{nms}\, \mathsf{J}\left(\breve{\psi}_m, \triangle_s \breve{\psi}_s\right) + \beta \partial_x \breve{\psi}_n = 0\,, \tag{36}$$

where

$$\Xi_{nms} \stackrel{\text{def}}{=} \frac{1}{h} \int_{z^-}^{z^+} \mathsf{p}_n \mathsf{p}_m \mathsf{p}_s \,\mathrm{d}z\,. \tag{37}$$

Note that $\Xi_{nms}$ cannot be computed exactly except in cases with simple buoyancy frequency profiles. But it suffices to compute $\Xi_{nms}$ to high accuracy, e.g. using Gaussian quadrature.

Flierl (1978) implicitly assumed that $\vartheta^+ = \vartheta^- = 0$, so that the surface terms in (22) vanish and then there is no difference between $q_{\mathrm{N}}^{A}$ and $q_{\mathrm{N}}^{\mathrm{G}}$. But in general, with nonzero surface buoyancy, we can append evolution equations for $\vartheta^+$ and $\vartheta^-$ to approximation A. That is, in addition to the $\mathrm{N}+1$ modal equations in (36), we also have

$$\partial_t \vartheta^{\pm} + \sum_{n=0}^{\mathrm{N}} \mathsf{p}_n^{\pm}\, \mathsf{J}(\breve{\psi}_n, \vartheta^{\pm}) = 0\,. \tag{38}$$

Above we have evaluated the $\psi$-series (15) at $z^{\pm}$ to approximate $\psi^{\pm}$ in the surface boundary conditions. This approach is not satisfactory because the resulting surface buoyancy equations (38) are dynamically passive i.e., $\vartheta^+$ and $\vartheta^-$ do not affect the interior evolution equations in (36).

Approximation A has the well-known energy conservation law

$$\frac{\mathrm{d}}{\mathrm{d}t}\sum_{n=0}^{\mathrm{N}}\int \tfrac{1}{2}(\nabla\breve{\psi}_n)^2+\tfrac{1}{2}\kappa_n^2\breve{\psi}_n^2\,\mathrm{d}S=0\,. \tag{39}$$

To obtain the energy analogous to $E$ in (10), the modal sum above is multiplied by the depth $h$. Approximation A also has the potential enstrophy conservation law,

$$\frac{\mathrm{d}}{\mathrm{d}t}\sum_{n=0}^{\mathrm{N}}\int \tfrac{1}{2}\left(\triangle_n\breve{\psi}_n\right)^2\mathrm{d}S=0\,. \tag{40}$$

But the analog of the exact potential enstrophy (12) is not conserved by A (nor by B and C below). Finally, with the surface equations in (38), approximation A also conserves surface buoyancy variance as in (13).

### *b. Approximation B*

Approximation B begins with the observation that the exact solution of the inversion problem in (19) and (20) can be decomposed as

$$\psi=\psi^I+\psi^S \tag{41}$$

where $\psi^I(x,y,z,t)$ is the "interior streamfunction" and $\psi^S(x,y,z,t)$ is the "surface streamfunction" (Lapeyre and Klein 2006; Tulloch and Smith 2009).

The surface streamfunction $\psi^S(x,y,z,t)$ is defined as the solution of the boundary value problem

$$\left(\triangle+\mathsf{L}\right)\psi^S=0\,, \tag{42}$$

with inhomogeneous Neumann boundary conditions

$$\left(\frac{f_0}{N}\right)^2\partial_z\psi^S\left(z^{\pm}\right)=\vartheta^{\pm}\,. \tag{43}$$

The interior streamfunction $\psi^I(x,y,z,t)$ is defined as the solution of the boundary value problem

$$\left(\triangle+\mathsf{L}\right)\psi^I=q\,, \tag{44}$$

with homogeneous Neumann boundary conditions

$$\left(\frac{f_0}{N}\right)^2 \partial_z \psi^I\left(z^{\pm}\right) = 0\,. \tag{45}$$

Approximation B assumes that one can solve the surface problem in (42) and (43) without resorting to truncated series. For instance, with constant or exponential stratifications one can find closed-form, exact expressions for $\psi^S$ (Tulloch and Smith 2009; LaCasce 2012). Approximation B requires that the two unknown Dirichlet boundary-condition functions $\psi^{S\pm} = \psi^S(z^{\pm})$ can be obtained efficiently from specified Neumann boundary-condition functions $\vartheta^+$ and $\vartheta^-$. The Eady problem, discussed below in section 5, is a prime example in which one can obtain this Neumann-to-Dirichlet map.

Once $\psi^S$ is in hand, the approximate streamfunction is

$$\psi_{\mathrm{N}}^B = \psi_{\mathrm{N}}^I + \psi^S\,, \tag{46}$$

where the approximate interior streamfunction $\psi_{\mathrm{N}}^I$ is obtained by solving the interior inversion problem (44) with the right hand side replaced by the N-mode Galerkin approximation $q_{\mathrm{N}}^{\mathrm{G}}$ defined in (17) and (18). The two-mode two-surface model of Tulloch & Smith (2009) is the case $\mathrm{N} = 1$. The exact solution of the approximate interior inversion problem is

$$\psi_{\mathrm{N}}^I = \sum_{n=0}^{\mathrm{N}} \breve{\psi}_n^I(x,y,t)\,\mathsf{p}_n(z)\,, \tag{47}$$

where

$$\breve{\psi}_n^I \stackrel{\text{def}}{=} \frac{1}{h}\int_{z^-}^{z^+} \mathsf{p}_n \psi^I \,\mathrm{d}z\,, \qquad \text{and} \qquad \triangle_n \breve{\psi}_n^I = \breve{q}_n\,. \tag{48}$$

To obtain the approximation B evolution equations we introduce the streamfunction (46) into the QGPV equation (6) and project onto mode $n$ to obtain

$$\begin{aligned}\partial_t \triangle_n \breve{\psi}_n + \sum_{m=0}^{\mathrm{N}} \sum_{s=0}^{\mathrm{N}} \Xi_{nms} \, \mathsf{J}\left(\breve{\psi}^I_m, \triangle_s \breve{\psi}^I_s\right) + \beta \partial_x \left(\breve{\psi}^I_n + \breve{\psi}^S_n\right) \\ + \sum_{s=0}^{\mathrm{N}} \tfrac{1}{h} \int_{z^-}^{z^+} \mathsf{p}_n \mathsf{p}_s \mathsf{J}\left(\psi^S, \triangle_s \breve{\psi}^I_s\right) \mathrm{d}z = 0\,,\end{aligned} \tag{49}$$

with $\Xi_{nms}$ defined in (37). Approximation B assumes that the remaining integral on the second line of (49) can be evaluated exactly. This is only possible for particular models of the $N(z)$ (e.g., constant buoyancy-frequency profiles). In practice, however, it may suffice to compute the integral on the second line (49) very accurately, e.g. using Gaussian quadrature.

The evolution equations for approximation B are completed with the addition of buoyancy-advection at the surfaces

$$\partial_t \vartheta^{\pm} + \mathsf{J}(\psi^{S\pm}, \vartheta^{\pm}) + \sum_{n=0}^{\mathrm{N}} \mathsf{p}^{\pm}_n \mathsf{J}(\breve{\psi}^I_n, \vartheta^{\pm}) = 0\,. \tag{50}$$

With (49) and (50) we have $\mathrm{N}+3$ evolution equations for the $\mathrm{N}+3$ fields $\breve{\psi}^I_0, \breve{\psi}^I_1, \cdots \breve{\psi}^I_{\mathrm{N}}$ and $\vartheta^{\pm}$.

Approximation B conserves surface buoyancy variance. But the conservation laws for energy is problematic: because $\psi^I$ is not orthogonal to $\psi^S$ the energy (10) is not conserved in approximation B (K.S. Smith personal communication). These non-conservative effects are quantitatively small, but are nonetheless irritating. The non-orthogonality of $\psi^I$ and $\psi^S$ was a motivation for development of the surface-aware modes by Smith & Vanneste (2013).

With $\beta = 0$, approximation B conserves potential enstrophy

$$\frac{\mathrm{d}}{\mathrm{d}t} \sum_{n=0}^{\mathrm{N}} \int \tfrac{1}{2} \left(\triangle_n \breve{\psi}^I_n\right)^2 \mathrm{d}S = 0\,. \tag{51}$$

But with $\beta \neq 0$ the analog of the exact potential enstrophy (12) is not conserved.

### *c. Approximation C*

Approximation C uses truncated Galerkin approximations $\psi_{\mathrm{N}}^{\mathrm{G}}$ and $q_{\mathrm{N}}^{\mathrm{G}}$ for *both* $\psi$ and $q$. The series $q_{\mathrm{N}}^{\mathrm{G}}$ is *not* obtained by differentiation of $\psi_{\mathrm{N}}^{\mathrm{G}}$ and therefore, as indicated in (24), the inversion equation is not satisfied exactly by $\psi_{\mathrm{N}}^{\mathrm{G}}$ and $q_{\mathrm{N}}^{\mathrm{G}}$. But instead, one will have true least-squares approximations to both $\psi$ and $q$. To our knowledge approximation C, correctly accounting for the surface-buoyancy boundary terms, has not been previously investigated.

Because method C approximates *both* the streamfunction and the PV by Galerkin series, the derivation of the modal equations is very straightforward compared with the calculations in appendix A of Flierl (1978): one simply substitutes the truncated Galerkin series for the streamfunction (15) and PV (17) into the QGPV equation (6), and then projects onto mode $n$ to obtain

$$\partial_t \breve{q}_n + \sum_{m=0}^{\mathrm{N}} \sum_{s=0}^{\mathrm{N}} \Xi_{nms} \, \mathsf{J}\left(\breve{\psi}_m, \breve{q}_s\right) + \beta \, \partial_x \breve{\psi}_n = 0 \,, \tag{52}$$

where $\Xi_{nms}$ is defined in (37), and we recall the relation between $\breve{\psi}_n$ and $\breve{q}_n$ from (22)

$$\breve{q}_n = \triangle_n \breve{\psi}_n + \tfrac{1}{h}\left(\mathsf{p}_n^+ \, \vartheta^+ - \mathsf{p}_n^- \, \vartheta^-\right) . \tag{53}$$

In approximation C there are $\mathrm{N}+3$ degrees of freedom: the $\mathrm{N}+1$ modal amplitudes $\breve{\psi}_n$ and the two surface buoyancy fields $\vartheta^{\pm}$. The approximation *C* evolution equations are completed by advection of the surface buoyancy

$$\partial_t \vartheta^{\pm} + \sum_{n=0}^{\mathrm{N}} \mathsf{p}_n^{\pm} \, \mathsf{J}(\breve{\psi}_n, \vartheta^{\pm}) = 0 \,. \tag{54}$$

We emphasize that in approximation C the surface buoyancy fields $\vartheta^{\pm}$ are not passive: $\breve{\psi}_n$, $\breve{q}_n$, and $\vartheta^{\pm}$ are related through (53).

Approximation C conserves surface buoyancy variance as in (13). Total energy is also conserved

$$\frac{\mathrm{d}}{\mathrm{d}t} \sum_{n=0}^{\mathrm{N}} \int \tfrac{1}{2} |\nabla \breve{\psi}_n|^2 + \tfrac{1}{2} \kappa_n^2 \breve{\psi}_n^2 \, \mathrm{d}S = 0 \,. \tag{55}$$

With $\beta = 0$, approximation C has a potential enstrophy conservation law

$$\frac{\mathrm{d}}{\mathrm{d}t}\sum_{n=0}^{\mathrm{N}}\int \tfrac{1}{2}\check{q}_n^2\,\mathrm{d}S = 0\,. \tag{56}$$

But with $\beta \neq 0$, as in B, approximation C does not conserve the analog of the exact potential enstrophy (12).

## 5. The Eady problem

We use classical linear stability problems with nonzero surface buoyancy to illustrate how solutions to specific problems can be constructed and to assess the relative merit and efficiency of approximations A, B, and C. The linear analysis does not provide the full picture of convergence of the approximate solutions. Nonetheless, in turbulence simulations forced by baroclinic instability, it is necessary (but not sufficient) to accurately capture the linear stability properties.

We use nondimensional variables so that the surfaces are at $z^+ = 0$ and $z^- = -1$. The Eady exact base-state velocity is given by (30) with zero PV $q = 0$ and $\beta = 0$.

### *a. Approximation A*

While the surface fields $\vartheta^\pm$ are dynamically passive in approximation A, the Eady problem can still be considered because the base-state PV defined via (35) converges to $\delta$-distributions on the boundaries (Section 3).

The base-state velocity in Approximation A is given by the series (31) and is a good approximation to the exact base-state velocity (30). But, according to approximation A, there is a nonzero interior base-state PV gradient given by the series (33). As $\mathrm{N} \to \infty$ the PV gradient in (33) converges in a distributional sense to Brethertonian sheets at $z = 0$ and $-1$. But for numerical implementation of approximation A we stop short of $\mathrm{N} = \infty$. While the PV gradient is much larger at the boundaries, there is always interior structure in the PV (Figure 1c). We show that this spurious interior PV gradient has a strong and unpleasant effect on the approximate solution of the Eady stability problem.

To solve the Eady linear stability we linearize the interior equations (36) about the base-state velocity in (31) and the PV gradient in (33). We assume $\breve{q}_k = \hat{q}_k \exp[\mathrm{i}(kx + ly - \omega^A t)]$, etc, to obtain a $(\mathrm{N}+1) \times (\mathrm{N}+1)$ eigenproblem

$$\sum_{m=0}^{\mathrm{N}} \sum_{s=0}^{\mathrm{N}} \Xi_{nms} \Big[ \breve{U}_m \hat{q}_s + \partial_y \breve{Q}_s \hat{\psi}_m \Big] = c^A \hat{q}_n, \tag{57}$$

where $\breve{Q}_s$ are the coefficients of the series (33) and $c^A \stackrel{\text{def}}{=} \omega^A / k$. The eigenproblem (57) can be recast in the matrix form $\mathsf{A}\mathsf{q} = c^A \mathsf{q}$, where $\tilde{\mathsf{q}} = [\hat{q}_0, \hat{q}_1, \ldots, \hat{q}_{\mathrm{N}-1}, \hat{q}_{\mathrm{N}}]^{\mathsf{T}}$ (Appendix B) and solved with standard methods.

Figure 2 shows the growth rate of the Eady instability according to approximation A, and compares this with the exact Eady growth rate. Approximation A does not do well, especially at large wavenumbers. The exact Eady growth rate has a high-wavenumber cut-off. At moderate values of N, such as 3, 5 and 7 approximation A produces unstable “bubbles” of instability at wavenumbers greater than the high-wavenumber cut-off. The growth rates in these bubbles are comparable to the true maximum growth rate. As N increases, the unstable bubbles are replaced by a long tail of unstable modes with a growth rate that slowly increases with $\kappa$. These spurious high-wavenumber instabilities are due to the rapidly oscillatory interior PV gradient which supports unphysical critical layers: see Figure 3.

### *b. Approximation B, the exact solution*

In approximation B, the zero PV in the Eady problem implies $\breve{q}_n = \breve{\psi}_n^I = 0$. The $\mathrm{N}+1$ modal equations (with $\beta = 0$) are trivially satisfied; there is no interior contribution ($\psi_{\mathrm{N}}^I = 0$). Thus approximation B solves the Eady problem exactly.

Assuming $\psi^S = \hat{\psi}^S(z)\exp[\mathrm{i}(kx+ly-\omega^B t)]$, we obtain the solution to the surface streamfunction inversion problem (42)-(43)

$$\hat{\psi}^S(z) = \frac{\cosh[\kappa(z+1)]}{\kappa\sinh\kappa}\,\vartheta^+ - \frac{\cosh(\kappa z)}{\kappa\sinh\kappa}\,\vartheta^-\,, \tag{58}$$

where the magnitude of the wavenumber vector is $\kappa = \sqrt{k^2+l^2}$. We evaluate the surface streamfunction (58) at the boundaries to find the relationship between the streamfunction at the surfaces $\hat{\psi^S}^{\pm}$ and the boundary fields $\vartheta^{\pm}$:

$$\begin{bmatrix} \hat{\psi^S}^+ \\ \hat{\psi^S}^- \end{bmatrix} = \frac{1}{\kappa}\begin{bmatrix} \coth\kappa & -\operatorname{csch}\kappa \\ \operatorname{csch}\kappa & -\coth\kappa \end{bmatrix}\begin{bmatrix} \hat{\vartheta}^+ \\ \hat{\vartheta}^- \end{bmatrix}, \tag{59}$$

The nondimensional linearized boundary conditions (50) are

$$\hat{\vartheta}^+ - \hat{\psi}^+ = c^B\hat{\vartheta}^+\,, \qquad \text{and} \qquad -\hat{\psi}^- = c^B\hat{\vartheta}^-\,, \tag{60}$$

where $c^B = \omega^B/k$. Using the boundary conditions (60) in (59) we obtain an eigenvalue problem

$$\underbrace{\frac{1}{\kappa}\begin{bmatrix} \kappa-\coth\kappa & \operatorname{csch}\kappa \\ -\operatorname{csch}\kappa & \coth\kappa \end{bmatrix}}_{\stackrel{\text{def}}{=}\mathsf{B}}\begin{bmatrix} \hat{\vartheta}^+ \\ \hat{\vartheta}^- \end{bmatrix} = c^B\begin{bmatrix} \hat{\vartheta}^+ \\ \hat{\vartheta}^- \end{bmatrix}. \tag{61}$$

The eigenvalues of $\mathsf{B}$ are given by the celebrated dispersion relation for the Eady problem (Pedlosky 1987; Vallis 2006)

$$c^B = \tfrac{1}{2} \pm \tfrac{1}{\kappa}\Big[\Big(\tfrac{\kappa}{2} - \tanh\tfrac{\kappa}{2}\Big)\Big(\tfrac{\kappa}{2} - \coth\tfrac{\kappa}{2}\Big)\Big]^{1/2}. \tag{62}$$

*c. Approximation C*

Approximation C expands both the streamfunction and the PV in standard vertical modes. Thus in the Eady problem the PV is exactly zero, as it should be: $q = \check{q}_n = 0$. Thus approximation C does not have the spurious critical layers that bedevil A. Moreover, in approximation C, the $\mathrm{N}+1$

modal equations (with $\beta = 0$) in (52) are trivially satisfied, and the inversion relationship (53) provides a simple connection between the streamfunction and the fields $\vartheta^{\pm}$. The base velocity for the Eady problem in approximation C is the series in (31) (the same as A). From the exact shear at the boundaries we obtain the exact base-state boundary variables

$$\Theta^{\pm} = -y\,. \tag{63}$$

We linearize the boundary equations (54) about the base-state (33) and (63), to obtain

$$\partial_t \vartheta^{\pm} + U_{\mathrm{N}}^{\mathrm{G}\pm} \partial_x \vartheta^{\pm} - \sum_{k=0}^{\mathrm{N}} \partial_x \breve{\psi}_k \mathsf{p}_k^{\pm} = 0\,. \tag{64}$$

Assuming $\vartheta^{\pm} = \hat{\vartheta}^{\pm} \exp[\mathrm{i}(kx + ly - \omega^C t)]$, and using the inversion relationship (53), we obtain a $2 \times 2$ eigenproblem

$$\mathsf{C} \begin{bmatrix} \hat{\vartheta}^{+} \\ \hat{\vartheta}^{-} \end{bmatrix} = c^C \begin{bmatrix} \hat{\vartheta}^{+} \\ \hat{\vartheta}^{-} \end{bmatrix}, \tag{65}$$

where matrix $\mathsf{C}$ is defined in appendix C. It is straightforward to show that $c^C$ converges to the exact eigenspeed. i.e., $c^C \to c^B$ as $\mathrm{N} \to \infty$ (Appendix C). Figure 2 shows that approximation C successfully captures the structure of the Eady growth rate even with modest values of N.

### *d. Remarks on convergence*

The crudest truncation (i.e. $\mathrm{N} = 0$) is stable for both approximations A and C (Figure 2). With one baroclinic mode ($\mathrm{N} = 1$) the growth rates ($\omega_i = k \times \mathrm{Im}\{c\}$) are qualitatively consistent with the exact solution, and the results improve with $\mathrm{N} = 2$. With a moderate number of baroclinic modes modes ($\mathrm{N} > 2$) approximations A and C converge rapidly to the exact growth rate at wavenumbers less than about 2.2 — see figure 2. But surprisingly the convergence of the growth rate at the most unstable mode ($\kappa \approx 1.6$) is faster in approximation A ($\sim \mathrm{N}^{-4}$) than in approximation C ($\sim\mathrm{N}^{-2}$) — see figure 4. However, the convergence in approximation C is uniform: there are no spurious high-wavenumber instabilities.

Figure 4 also shows that the approximation A convergence of the growth rate to zero at $\kappa = 8$ is slow ($\sim\mathrm{N}^{-1}$). While the growth rate does converge to zero at a fixed wavenumber, such as $\kappa = 8$, we conjecture that there are always faster growing modes at larger wavenumbers.

## 6. The Green problem

To further explore the relative merit and efficiency of approximations A, B, and C we study the instability properties of a system with nonzero $\beta$. For simplicity, we consider a problem with Eady's base-state $\psi = -(1+z)y$ on a $\beta$-plane. This is similar to the problem originally considered by Charney (1947) and Green (1960). The major difference is that Charney considered a vertically semi-infinite domain (Charney 1947; Pedlosky 1987) while we follow Green and consider a finite-depth domain with $-1 < z < 0$.

We obtain the exact system for this "Green problem" by linearizing the QG equations (6)-(9) about the base-state (30) with background PV $\beta y$, where $\hat{\beta}$ is the nondimensional planetary PV gradient. Assuming $\psi = \hat{\psi}\exp[\mathrm{i}(kx + ly - \omega t)]$, we obtain

$$(U-c)\left[\hat{\psi}_{zz} - \kappa^2\hat{\psi}\right] + \hat{\beta}\,\hat{\psi} = 0\,, \qquad -1 < z < 0\,, \tag{66}$$

and

$$(U-c)\,\hat{\psi}_z - \hat{\psi} = 0\,, \qquad z = -1\,,0\,. \tag{67}$$

As a reference solution, we solve the eigenproblem (66)-(67) using a centered second-order finite-difference scheme with 1000 vertical levels: see Figure 5.

The Green problem supports three classes of unstable modes, indicated in the lower right panel ($\mathrm{N} = 128$) of Figure 5: (1) the "modified Eady modes", which are instabilities that arise from the interaction of Eady-like edge waves, only slightly modified by $\beta$; (2) the "Green modes", which are very long slowly growing modes (Vallis 2006); (3) the high-wavenumber "Charney modes" are critical layer instabilities that arise from the interaction of the surface edge wave with the interior Rossby wave that is supported by nonzero $\beta$.

### *a. Implementation of approximation A*

The base-state for the Green problem is the same as in the Eady problem. In approximation A, the $\beta$-term adds only a diagonal term to the Eady system (57) (see appendix C).

### *b. Implementation of approximation B*

The base-state is the same as in the Eady problem. The steady streamfunction and buoyancy fields that satisfy (49) and (50) exactly are

$$\Sigma = -(1+z)\,y \qquad \text{and} \qquad \Theta^{\pm} = -y\,. \tag{68}$$

Assuming $\breve{q}_n = \hat{q}_n(z)\exp[\mathrm{i}(kx+ly-\omega^B t)]$, the $\mathrm{N}+1$ interior equations (49) linearized about (68) are

$$\sum_{s=0}^{\mathrm{N}} \xi_{ns}\hat{q}_s + \hat{\beta}\left(\hat{\psi}_n + \hat{\psi}_n^S\right) = c_c^B\,\hat{q}_n\,, \tag{69}$$

where

$$\xi_{ns} \overset{\mathrm{def}}{=} \frac{1}{h}\int_{z^-}^{z^+} \mathsf{p}_n\,\mathsf{p}_s\,(z+1)\,\mathrm{d}z\,. \tag{70}$$

The boundary conditions (50), linearized about (68), are

$$\hat{\vartheta}^+ - \sum_{s=0}^{\mathrm{N}} \mathsf{p}_s^+\,\hat{\psi}_s - \hat{\psi}^S + = c_c^B\,\hat{\vartheta}^+\,, \tag{71}$$

and

$$-\sum_{s=0}^{\mathrm{N}} \mathsf{p}_s^-\,\hat{\psi}_s - \hat{\psi}^S - = c_c^B\,\hat{\vartheta}^-\,, \tag{72}$$

where $\hat{\psi}^S$ is given by (58). We use the inversion relationship (48) and the Neumann-to-Dirichlet map (59) to recast this eigenproblem into standard form $\mathsf{B}\tilde{\mathsf{q}} = c^B\tilde{\mathsf{q}}$, where $\tilde{\mathsf{q}} = [\hat{\vartheta}^+, \hat{q}_0, \hat{q}_1, \ldots, \hat{q}_{\mathrm{N}-1}, \hat{q}_{\mathrm{N}}, \hat{\vartheta}^-]^\mathsf{T}$ (see appendix C).

### *c. Implementation of approximation C*

Again the base-state is the same as in the Eady problem. But now there are $\mathrm{N}+3$ equations: the two boundary equations of Eady's problem (64) plus $\mathrm{N}+1$ interior equations

$$\sum_{m=0}^{\mathrm{N}}\sum_{s=0}^{\mathrm{N}} \Xi_{nms}\breve{U}_m\,\hat{q}_s + \hat{\beta}\,\hat{\psi}_n = c^C\hat{q}_n\,, \tag{73}$$

We use the inversion relationship (53) in (73) to recast this eigenproblem in the form $\mathsf{C}\tilde{\mathsf{q}} = c^C\tilde{\mathsf{q}}$, where $\tilde{\mathsf{q}}$ is defined as in approximation B (see appendix C).

### *d. Remarks on convergence*

The most crude truncation ($\mathrm{N}=0$) is stable for approximations A and C. In contrast, the $\mathrm{N}=0$ truncation in approximation B is qualitatively consistent with the modified Eady instabilities: see figure 5. With a moderate number of baroclinic modes ($\mathrm{N}=2$ or 3), approximations A, B and C all resolve the modified Eady modes relatively well. At the most unstable modified Eady mode ($\kappa \approx 1.9$), approximation B has typically the smallest error because it solves the surface problem exactly. As in the Eady problem, approximation A converges ($\sim \mathrm{N}^{-4}$) faster than approximations B and C ($\sim \mathrm{N}^{-2}$) at the most unstable mode, but B and C converge faster at high wavenumbers.

Approximations A, B, and C all converge very slowly to the high-wavenumber Charney modes (Figures 5 and 6). These modes are interior critical-layer instabilities (Pedlosky 1987) and the critical layer is confined to a small region about the steering level (i.e., the depth at which the phase speed matches the base velocity — see figure 7). With finite base-state shear, the critical layer is always in the interior. Thus, the problem is not that standard vertical modes are inefficient because they do not satisfy inhomogeneous boundary conditions; a low resolution finite-difference solution also presents such "bubbles" in high-wavenumber growth rates (not shown). Resolution of the interior critical layer, not the surface boundary condition, is a problem for all methods at high wavenumbers. The "surface-aware" modes of Smith and Vanneste (2013) have similar performance to approximations B and C, but also have the same limitation — a large number of vertical modes is required to resolve interior critical layers (K. S. Smith, personal communication).

For example, with $\mathrm{N} < 25$, at $\kappa = 8$, approximations are qualitatively inconsistent with the high-resolution finite-difference solution. For larger values of N, the growth rate convergence for approximations B and C scales $\sim \mathrm{N}^{-3}$. The growth rate for approximation A converges painfully slowly ($\sim \mathrm{N}^{-1}$). As in the Eady problem, at large wavenumbers, the growth rate for approximation A is qualitatively different from that of the finite-difference solution because of spurious instabilities associated with the rapidly oscillatory base-state PV gradient in (33).

## 7. Summary and conclusions

The Galerkin approximations A, B, and C are equivalent if there are no buoyancy variations at the surfaces. Thus all three approximations are well-suited for applications with zero surface buoyancy (Flierl 1978; Fu and Flierl 1980; Hua and Haidvogel 1986). But with nonzero surface buoyancy the three approximations are fundamentally different. In particular, approximation A, originally introduced by Flierl (1978) in a context without surface buoyancy, obtains the approximate PV by differentiating the Galerkin series for the streamfunction, and consequently its approximate PV has violent oscillations in the interior. Approximation B represents the PV as a Galerkin series in standard modes and calculates the streamfunction that satisfies the exact inversion problem associated with the approximate PV (Tulloch and Smith 2009). The inversion relationship is split into surface and interior problems. Because the surface streamfunction projects onto the interior solution the energy is not diagonalized and consequently approximation B has small errors in energy conservation (K.S. Smith personal communication). The surface-aware modes of Smith & Vanneste (2013) correct this problem. Approximation C uses Galerkin series for both streamfunction and PV but does not satisfy the inversion problem exactly. Nevertheless, the Galerkin series for $\psi$ and $q$ converge absolutely and uniformly, and approximation C provides a good finite truncation of the QG equations that represents surface buoyancy dynamics and also conserves energy.

With nonzero interior PV gradients the convergence of all approximations is slow for the high-wavenumber Charney-type modes. The critical layer associated with these modes spans a very small fraction of the total depth (Figure 7). To accurately resolve these near-singularities at the steering level there is no better solution than having high vertical resolution in the interior.

For problems with nonuniform surface buoyancy and nonzero interior PV gradient, we recommend approximation C for obtaining solutions to the three-dimensional QG equations using standard vertical modes.

The codes that produced the numerical results of this paper, plotting scripts, and supplementary figures are openly available at `github.com/crocha700/qg_vertical_modes`.

*Acknowledgments.* CBR is grateful for a helpful conversation with G. R. Flierl. We thank Joe LaCasce and Shafer Smith for reviewing this paper. We had useful discussions with Shafer Smith regarding approximation B and the "surface-aware" modes, and with Geoff Vallis — who pointed out that Green (1960) first considered the Eady+$\beta$ problem. This research was supported by the National Science Foundation under award OCE 1357047.

## APPENDIX A

## Convergence of Galerkin series in standard modes

Jackson (1914) gives conditions for the uniform convergence of series expansions in eigenfunctions of the Sturm-Liouville eigenproblem

$$\frac{\mathrm{d}^2\mathsf{P}_n}{\mathrm{d}Z^2} + \left[\rho_n^2 - \Lambda(Z)\right]\mathsf{P}_n = 0\,, \tag{A1}$$

defined on the interval $Z \in [0, \pi]$ with boundary conditions

$$\mathsf{P}_n'(0) - \gamma_0 \mathsf{P}_n(0) = 0\,, \text{ and } \mathsf{P}_n'(\pi) - \gamma_\pi \mathsf{P}_n(\pi) = 0 \tag{A2}$$

where $\gamma_0$ and $\gamma_\pi$ are real constants of arbitrary sign and $\rho_n^2$ is the eigenvalue. The equations defining the standard modes (1)-(2) can be brought to this form using the following Liouville transformation

$$Z(z) = \frac{1}{\bar{Z}}\int_{z^-}^{z} S(\xi)^{-1/2}\mathrm{d}\xi\,, \text{ with } \bar{Z} \stackrel{\text{def}}{=} \frac{1}{\pi}\int_{z^-}^{z^+} S(\xi)^{-1/2}\mathrm{d}\xi\,, \tag{A3}$$

and

$$\mathsf{P}_n(Z) = S(z)^{1/4}\mathsf{p}_n(z)\,, \quad \text{where} \quad S(z) \stackrel{\text{def}}{=} \frac{f_0^2}{N^2(z)}\,. \tag{A4}$$

The eigenvalues are related by $\rho_n = \bar{Z}\kappa_n$ and

$$\Lambda(Z) = \bar{Z}^2\left[\frac{1}{4}\frac{\mathrm{d}^2 S}{\mathrm{d}z^2} - \frac{1}{16S}\left(\frac{\mathrm{d}S}{\mathrm{d}z}\right)^2\right]. \tag{A5}$$

The boundary condition for the standard modes (2) implies that the transformed modes satisfy (A2) with

$$\gamma_0 = \frac{4S(z^-)^{1/2}}{\bar{Z}\mathrm{d}S(z^-)/\mathrm{d}z}\,, \quad \text{and} \quad \gamma_\pi = -\frac{4S(z^+)^{1/2}}{\bar{Z}\mathrm{d}S(z^+)/\mathrm{d}z}\,. \tag{A6}$$

If $\mathrm{d}S/\mathrm{d}z = 0$ at a boundary then the appropriate condition at that boundary is $P_n = 0$.

A special case of Theorem I from Jackson (1914) states that the expansion of a function $f(Z)$ as a series in eigenfunctions $\mathsf{P}_n$ converges absolutely and uniformly provided that both $\mathrm{d}f/\mathrm{d}Z$ and $\mathrm{d}\Lambda/\mathrm{d}Z$ are continuous and bounded, regardless of whether or not $f$ satisfies the same boundary conditions as $\mathsf{P}_n$. (The remainder of the theorem concerns the rate of convergence under stronger conditions on $\psi$ and $\Lambda$.) The streamfunction, potential vorticity, and buoyancy profiles are typically assumed to be smooth in studies of QG dynamics, which implies that both $f$ and $\Lambda$ will satisfy the above conditions. Uniform convergence over $Z \in [0,\pi]$ implies uniform convergence over $z \in [z^-, z^+]$.

## APPENDIX B

## Derivation of conservation laws for approximation C

To obtain the conservation of energy in approximation C we multiply the modal equations (52) by $-\breve{\psi}_n$, integrate over the horizontal surface, and sum on $n$, to obtain

$$\begin{aligned}
&\frac{\mathrm{d}}{\mathrm{d}t}\sum_{n=0}^{\mathrm{N}}\int\left[(\nabla\breve{\psi}_n)^2+\kappa_n^2\breve{\psi}_n^2\right]\mathrm{d}S\\
&\quad-\sum_{n=0}^{\mathrm{N}}\frac{1}{h}\int\breve{\psi}_n\partial_t\left(\mathsf{p}_n^+\vartheta^+-\mathsf{p}_n^-\vartheta^-\right)\mathrm{d}S\\
&\quad+\sum_{n=0}^{\mathrm{N}}\sum_{m=0}^{\mathrm{N}}\sum_{s=0}^{\mathrm{N}}\Xi_{nms}\int\breve{\psi}_n\,\mathsf{J}\left(\breve{\psi}_m,\triangle_s\breve{\psi}_s\right)\mathrm{d}S=0\,,
\end{aligned}\tag{B1}$$

The triple sum term vanishes by the same symmetry arguments used above in approximation A. The term on the second line of (B1) is also zero: multiply the boundary conditions (54) by $\mathsf{p}_n^{\pm}\,\breve{\psi}_n$ and integrate over the horizontal surface. Thus we obtain the energy conservation law in (55).

The analog of the exact potential enstrophy (12),

$$Z_n \stackrel{\text{def}}{=} \sum_{n=0}^{\mathrm{N}}\int\frac{\breve{q}_n^2}{2}+\breve{q}_n\triangle_n\breve{\psi}_n\mathrm{d}S\,,\tag{B2}$$

is only conserved with $\mathrm{N}=0$.

## APPENDIX C

## Details of the stability problems

*a. The interaction tensor*

Because the standard vertical modes with constant stratification are simple sinusoids (29), the interaction coefficients (37) can be computed analytically. First we recall that $\Xi_{ijk}$ is fully symmetric. Permuting the indices so that $i \geq j \geq k$ we obtain

$$\Xi_{ijk} = \begin{cases} 1: & i = j, k = 0; \\ \frac{\sqrt{2}}{2}: & i = j + k; \\ 0: & \text{otherwise}. \end{cases} \tag{C1}$$

The second line in (C1) corrects a factor of $\frac{1}{2}$ missed by Hua and Haidvogel (1986).

*b. Approximation A*

Using the symmetry in $\Xi_{nms}$, and the inversion relation (35), we rewrite row $n+1$ of the linear Green system

$$\sum_{s=0}^{\mathrm{N}} \sum_{m=0}^{\mathrm{N}} \Xi_{nms} \left( \breve{U}_m + \partial_y \breve{Q}_m \, \alpha_s \right) \hat{q}_s + \hat{\beta} \, \alpha_n \hat{q}_n = c^A \hat{q}_n, \tag{C2}$$

where the inverse of the $n$'th mode Helmholtz operator in Fourier space is

$$\alpha_n \stackrel{\text{def}}{=} -(\kappa^2 + (n\pi)^2)^{-1} \,. \tag{C3}$$

The Eady problem is the special case $\hat{\beta} = 0$. We use a standard eigenvalue-eigenvector algorithm to obtain the approximate eigenspeed $c^A$.

*c. Approximation B*

The Green eigenvalue problem in (69) through (72) can be recast in the standard form $\mathsf{B}\,\mathsf{q} = c^B\,\mathsf{q}$, where $\tilde{\mathsf{q}} = [\hat{\vartheta^+}, \hat{q}_0, \hat{q}_1, \ldots, \hat{q}_{\mathrm{N}-1}, \hat{q}_{\mathrm{N}}, \hat{\vartheta^-}]^{\mathsf{T}}$. The first and last rows of the system stem from the boundary conditions (71)-(72)

$$\left(1-\frac{\coth\kappa}{\kappa}\right)\hat{\vartheta}^{+}-\sum_{s=0}^{\mathrm{N}}\mathsf{p}_s^{+}\alpha_s\hat{q}_s-\frac{\operatorname{csch}\kappa}{\kappa}\,\hat{\vartheta}^{-}=c^{B}\,\hat{\vartheta}^{+}\,, \tag{C4}$$

and

$$\frac{\operatorname{csch}\kappa}{\kappa}\,\hat{\vartheta}^{+}-\sum_{s=0}^{\mathrm{N}}\mathsf{p}_s^{-}\,\alpha_s\,\hat{q}_s+\frac{\coth\kappa}{\kappa}\,\hat{\vartheta}^{-}=c^{B}\,\hat{\vartheta}^{-}\,. \tag{C5}$$

The $(n+1)$'th row originates from the $n$'th interior equation (69)

$$-\hat{\beta}\,\mathsf{p}_n^{+}\,\alpha_n\,\vartheta^{+}+\sum_{s=0}^{\mathrm{N}}\gamma_{ns}\hat{q}_s+(\beta\,\alpha_n+1)+\hat{\beta}\,\mathsf{p}_n^{-}\,\alpha_n\,\vartheta^{-}=c^{B}\,\hat{q}_n\,, \tag{C6}$$

where the symmetric matrix $\gamma_{ms}$ is

$$\gamma_{ij}\stackrel{\text{def}}{=}\int_{-1}^{0}\mathsf{p}_i\,\mathsf{p}_j\,z\,\mathrm{d}z=\begin{cases}-\frac{1}{2}: & i=j\,;\\[2ex] \frac{2\sqrt{2}}{(j\pi)^2}: & i=0,\ j\ \text{ is odd}\,;\\[2ex] \frac{4\left(i^2+j^2\right)}{\left[\left(i^2-j^2\right)\pi\right]^2}: & i+j\ \text{ is odd}\,.\end{cases} \tag{C7}$$

*d. Approximation C*

THE EADY PROBLEM

The $2\times2$ eigenproblem is

$$\underbrace{\begin{bmatrix}U_{\mathrm{N}}^{\mathrm{G}+}+\Sigma_{\mathrm{N}} & -\Omega_{\mathrm{N}}\\[1ex] \Omega_{\mathrm{N}} & U_{\mathrm{N}}^{\mathrm{G}-}-\Sigma_{\mathrm{N}}\end{bmatrix}}_{\stackrel{\text{def}}{=}\mathsf{C}}\begin{bmatrix}\hat{\vartheta}^{+}\\[1ex] \hat{\vartheta}^{-}\end{bmatrix}=c^{C}\begin{bmatrix}\hat{\vartheta}^{+}\\[1ex] \hat{\vartheta}^{-}\end{bmatrix}, \tag{C8}$$

where

$$\Sigma_{\mathrm{N}}\stackrel{\text{def}}{=}\alpha_0+2\sum_{n=1}^{\mathrm{N}}\alpha_n\,,\quad\text{and}\quad\Omega_{\mathrm{N}}\stackrel{\text{def}}{=}\alpha_0+2\sum_{n=1}^{\mathrm{N}}(-1)^n\alpha_n\,. \tag{C9}$$

The sums (C9) become exact in the limit $\mathrm{N}\to\infty$

$$\Sigma_{\infty}=-\frac{\coth\kappa}{\kappa}\,,\qquad\text{and}\qquad\Omega_{\infty}=-\frac{\operatorname{csch}\kappa}{\kappa}\,. \tag{C10}$$

The base velocity also converges to the exact result. Using standard results for the summation of inverse squares, we obtain

$$U_\infty^{\mathrm{G}+} = 1\,, \qquad \text{and} \qquad U_\infty^{\mathrm{G}-} = 0\,. \tag{C11}$$

Thus

$$\mathsf{C} \to \mathsf{B} \qquad \text{as} \qquad \mathrm{N} \to \infty\,, \tag{C12}$$

and the eigenvalues of the Eady problem using approximation C become exact i.e., $c^C \to c^B$ as $\mathrm{N} \to \infty$.

THE GREEN PROBLEM

The $(\mathrm{N}+3) \times (\mathrm{N}+3)$ eigenproblem is

$$\mathsf{C}\,\tilde{\mathsf{q}} = c^C\,\tilde{\mathsf{q}}\,, \tag{C13}$$

where $\tilde{\mathsf{q}}$ is defined as above in approximation B. The first and last rows of (C13) stem from the boundary conditions (64)

$$\left(U_\mathrm{N}^{\mathrm{G}+} + \Sigma_\mathrm{N}\right)\hat{\vartheta}^+ - \sum_{n=0}^{\mathrm{N}} \alpha_n \mathsf{p}_n^+ \hat{q}_n - \Omega_\mathrm{N}\hat{\vartheta}^- = c^C\hat{\vartheta}^+\,, \tag{C14}$$

and

$$\Omega_\mathrm{N}\hat{\vartheta}^+ - \sum_{n=0}^{\mathrm{N}} \alpha_n \mathsf{p}_n^- \hat{q}_n + \left(U_\mathrm{N}^{\mathrm{G}-} - \Sigma_\mathrm{N}\right)\hat{\vartheta}^- = c^C\hat{\vartheta}^-\,. \tag{C15}$$

Row $n+1$ originates from the $n$'th modal equation (73):

$$\begin{aligned} \hat{\beta}\,\alpha_n \mathsf{p}_n^+\,\hat{\vartheta}^+ + \sum_{s=0}^{\mathrm{N}}\sum_{m=0}^{\mathrm{N}} \Xi_{mns}\breve{U}_m\hat{q}_s + \hat{\beta}\,\alpha_n\,\hat{q}_n& \\ -\hat{\beta}\,\alpha_n \mathsf{p}^-\,\hat{\vartheta}^- = c^C\hat{q}_n\,.& \end{aligned} \tag{C16}$$

## References


Bretherton, F., 1966: Critical layer instability in baroclinic flows. *Quarterly Journal of the Royal Meteorological Society*, **92 (393)**, 325–334.

Callies, J., G. Flierl, R. Ferrari, and B. Fox-Kemper, 2015: The role of mixed layer instabilities in submesoscale turbulence. *Journal of Fluid Mechanics*, submitted.

Charney, J. G., 1947: The dynamics of long waves in a baroclinic westerly current. *Journal of Meteorology*, **4 (5)**, 136–162.

Charney, J. G., 1971: Geostrophic turbulence. *Journal of the Atmospheric Sciences*, **28 (6)**, 1087–1095.

Ferrari, R., and C. Wunsch, 2010: The distribution of eddy kinetic and potential energies in the global ocean. *Tellus A*, **62 (2)**, 92–108.

Flierl, G. R., 1978: Models of vertical structure and the calibration of two-layer models. *Dynamics of Atmospheres and Oceans*, **2 (4)**, 341–381.

Fu, L.-L., and G. R. Flierl, 1980: Nonlinear energy and enstrophy transfers in a realistically stratified ocean. *Dynamics of Atmospheres and Oceans*, **4 (4)**, 219–246.

Gill, A. E., 1982: *Atmosphere-Ocean Dynamics*, Vol. 30. Academic press.

Green, J., 1960: A problem in baroclinic stability. *Quarterly Journal of the Royal Meteorological Society*, **86 (368)**, 237–251.

Hua, B., and D. Haidvogel, 1986: Numerical simulations of the vertical structure of quasi-geostrophic turbulence. *Journal of the atmospheric sciences*, **43 (23)**, 2923–2936.

Hunter, J. K., and B. Nachtergaele, 2001: *Applied Analysis*. World Scientific.

Jackson, D., 1914: On the degree of convergence of Sturm-Liouville series. *Transactions of the American Mathematical Society*, **15 (4)**, 439–466.

LaCasce, J., 2012: Surface quasigeostrophic solutions and baroclinic modes with exponential stratification. *Journal of Physical Oceanography*, **42 (4)**, 569–580.

Lapeyre, G., 2009: What vertical mode does the altimeter reflect? on the decomposition in baroclinic modes and on a surface-trapped mode. *Journal of Physical Oceanography*, **39 (11)**, 2857–2874.

Lapeyre, G., and P. Klein, 2006: Dynamics of the upper oceanic layers in terms of surface quasi-geostrophy theory. *Journal of physical oceanography*, **36 (2)**, 165–176.

Pedlosky, J., 1987: *Geophysical Fluid Dynamics, 1987*. Springer-Verlag, New York.

Roullet, G., J. McWilliams, X. Capet, and M. Molemaker, 2012: Properties of steady geostrophic turbulence with isopycnal outcropping. *Journal of Physical Oceanography*, **42 (1)**, 18–38.

Smith, K. S., and J. Vanneste, 2013: A surface-aware projection basis for quasigeostrophic flow. *Journal of Physical Oceanography*, **43 (3)**, 548–562.

Tulloch, R., and K. S. Smith, 2009: Quasigeostrophic turbulence with explicit surface dynamics: Application to the atmospheric energy spectrum. *Journal of the Atmospheric Sciences*, **66 (2)**, 450–467.

Vallis, G. K., 2006: *Atmospheric and Oceanic Fluid Dynamics: Fundamentals and Large-scale Circulation*. Cambridge University Press.

# LIST OF FIGURES

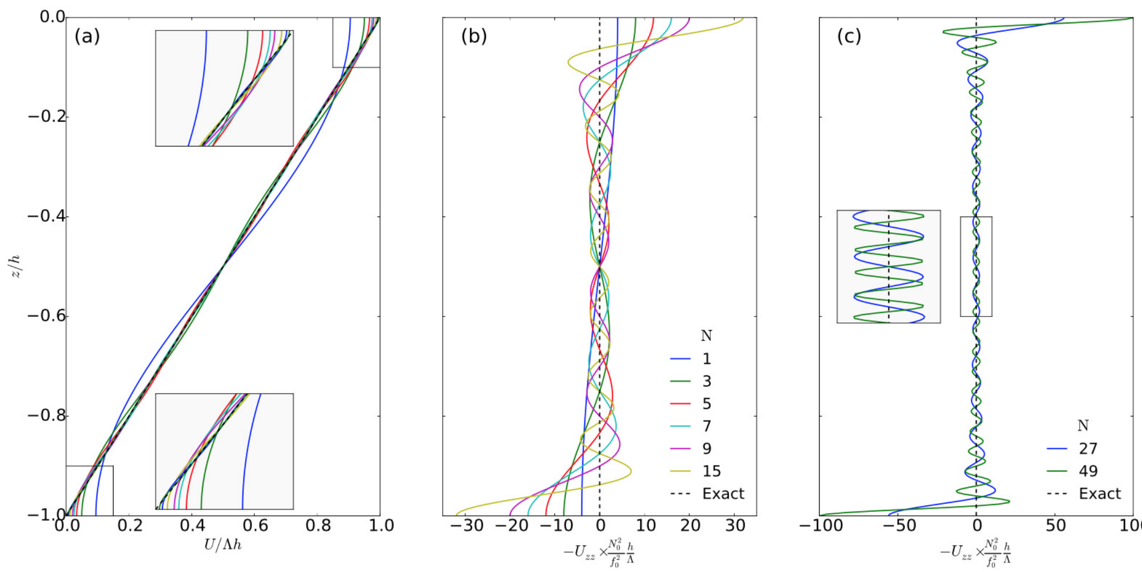


FIG. 1. Nondimensional base-state for the Eady problem using various truncation for the series (31). In the middle panel N is the number of baroclinic modes. (a) Zonal velocity: although the truncation has zero slope at the boundaries there are no Gibbs oscillations. (b) Meridional PV gradient associated with the truncated series (33). (c) as in (b) but with an expanded abscissa. As N increases, the PV gradient distributionally converges to two Brethertonian delta functions at the boundaries.

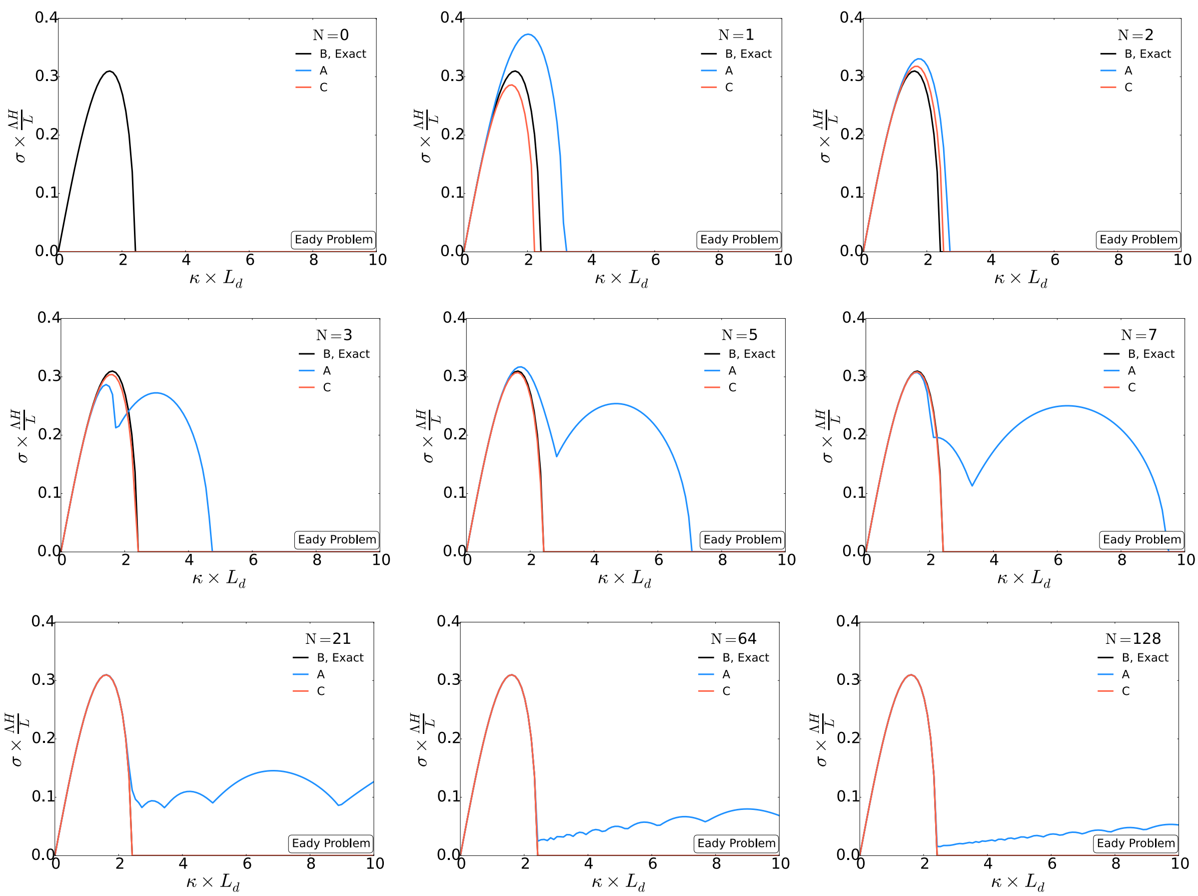


FIG. 2. Growth rate for the Eady problem as a function of the zonal wavenumber ($l = 0$) using approximations A, B (exact), C with various number of baroclinic modes (N).

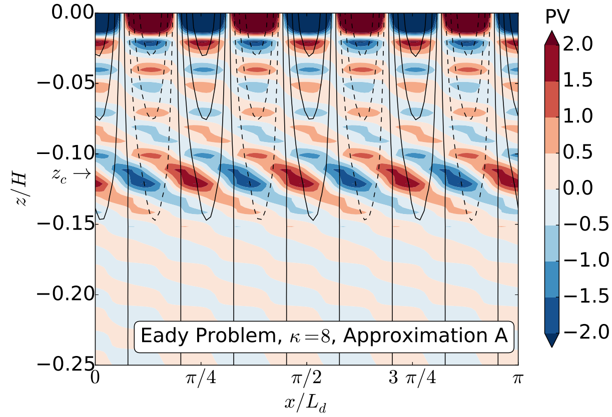


FIG. 3. Structure of $\kappa = 8$ unstable mode for the Eady problem obtained using approximation A and $\mathrm{N} = 64$. Streamfunction is the black curves and PV is the colors. The streamfunction slightly tilts westward as $z$ increases. One can see the unphysical critical layer associated with the fast-oscillating base-state PV. The critical level, $z_c$, is the depth where the unstable wave speed matches the velocity of the base-state. Only the top quarter of the domain is shown.

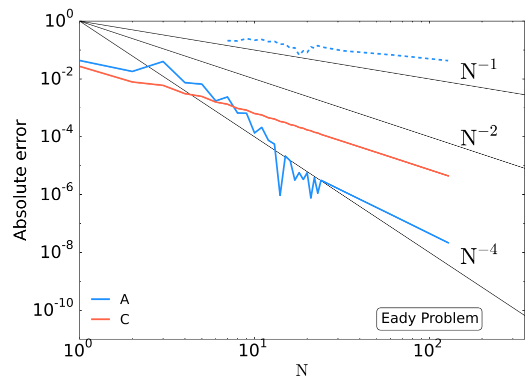


FIG. 4. Absolute error as a function of number of baroclinic modes (N) for the growth rates of the Eady problem. The solid lines show the error at the exact fastest growing mode ($\kappa \approx 1.6$). The dashed line is the approximation A error at $\kappa = 8$.

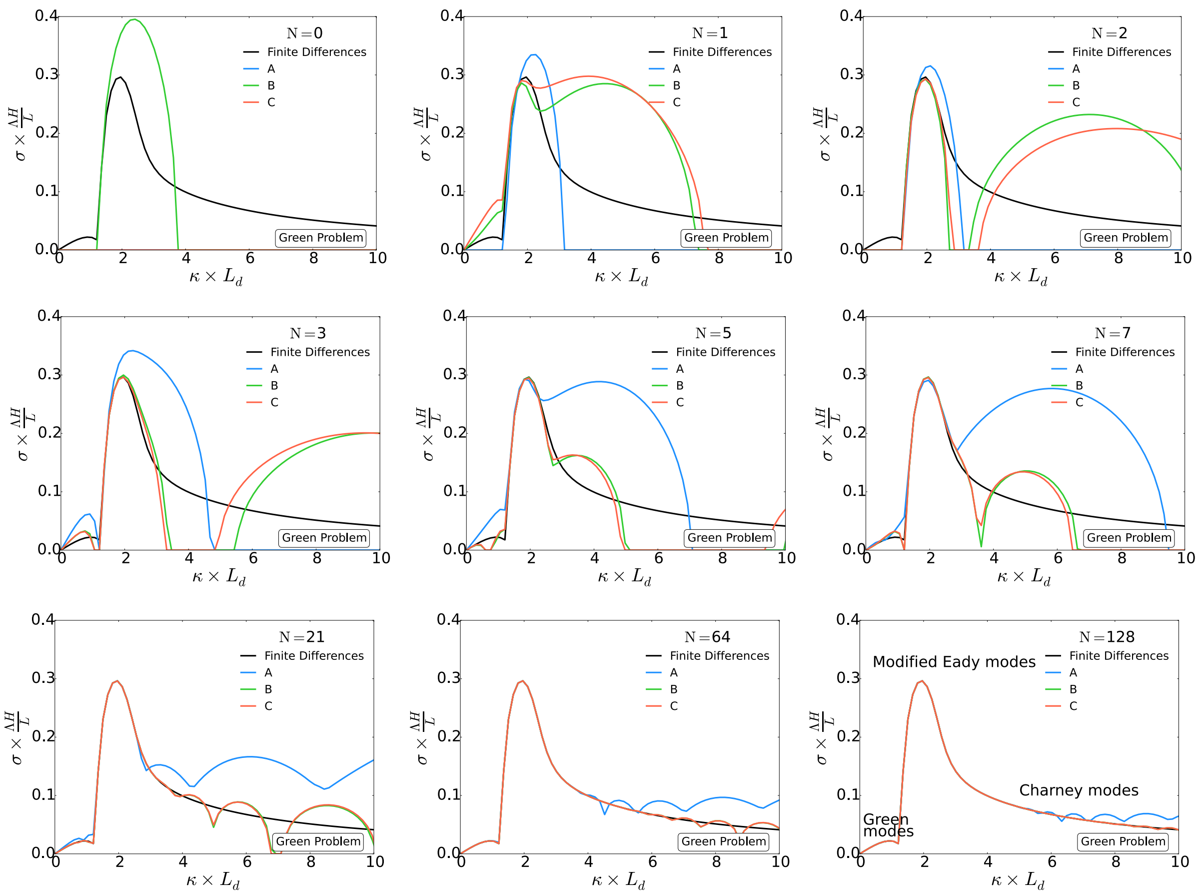


FIG. 5. Growth rate for the Green problem with $\hat{\beta} = 1$ as a function of the zonal wavenumber ($l = 0$) using approximations A, B, C with various number of baroclinic modes (N). The black line is a finite-differences solution with 1000 vertical levels.

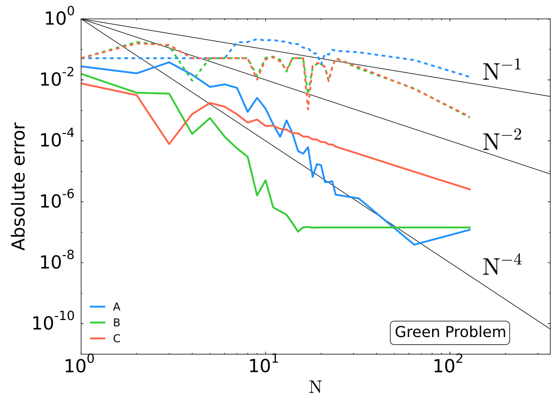


616 FIG. 6. Absolute error as a function of number of baroclinic modes (N) for the growth rates of the Green problem. The solid line represent the error at the exact fastest growing mode ($\kappa \approx 1.9$). The dashed line is the error at $\kappa = 8$.

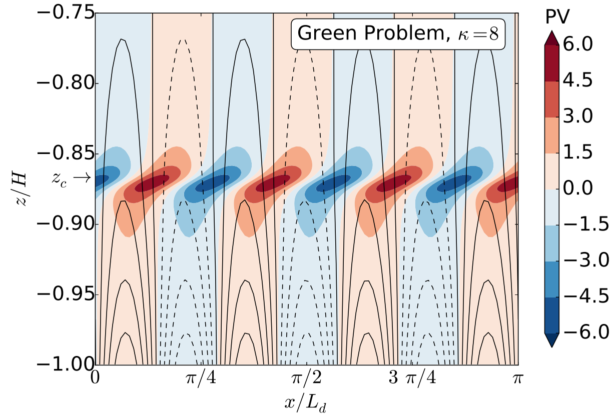


FIG. 7. Wave structure of the $\kappa = 8$ unstable mode for the Green problem with $\hat{\beta} = 1$ solved using a second-order finite-difference scheme with 1000 vertical levels. Streamfunction (black contours) and potential vorticity (colors). The streamfunction slightly tilts westward as $z$ increases. The potential vorticity is confined to a small region, the critical layer. The critical level, $z_c$, is the depth where the unstable wave speed matches the velocity of the base-state. Only the bottom quarter of the domain is shown.